

Linkages between Tropopause Polar Vortices and the Great Arctic Cyclone of August 2012

**Daniel Keyser¹, Kevin A. Biernat¹, Lance F. Bosart¹,
and Steven M. Cavallo²**

*¹Department of Atmospheric and Environmental Sciences
University at Albany, State University of New York*

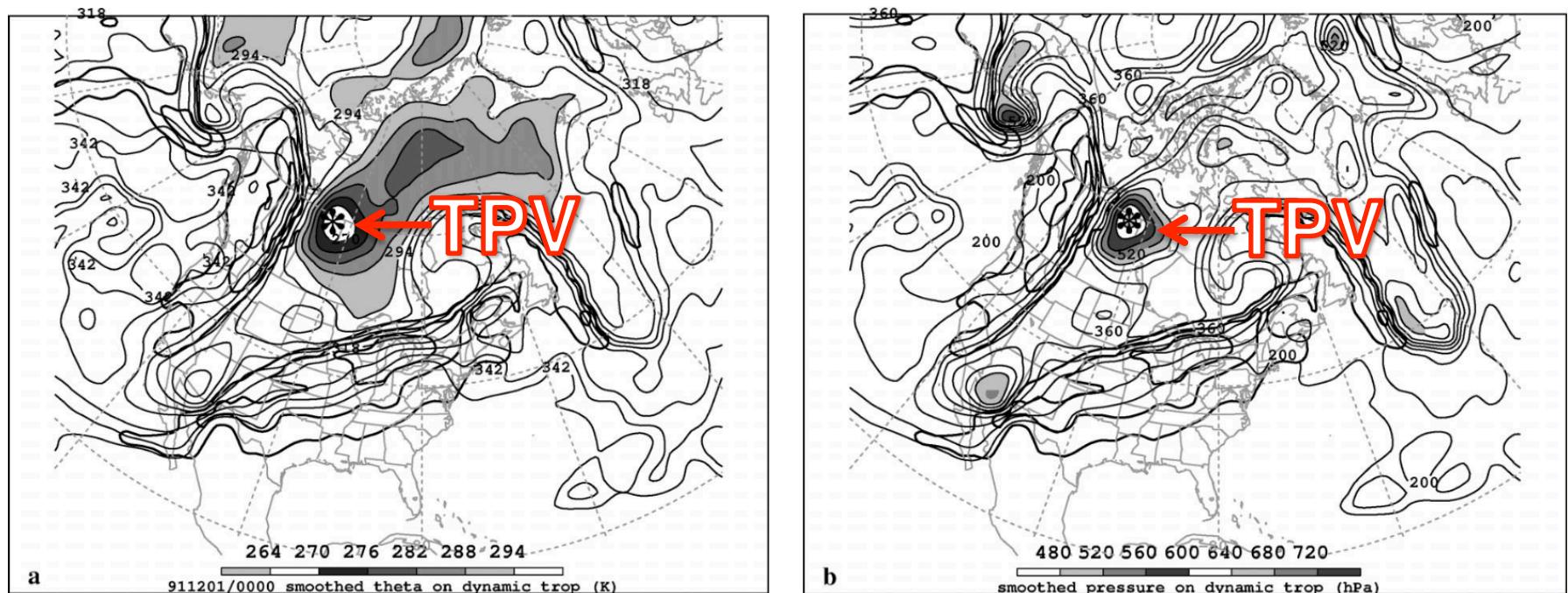
²University of Oklahoma

Department of Atmospheric and Oceanic Sciences
McGill University
Monday 28 January 2019

Research Supported by ONR Grant N00014-18-1-2200

What are Tropopause Polar Vortices (TPVs)?

- TPVs are defined as tropopause-based vortices of high-latitude origin and are material features (Pyle et al. 2004; Cavallo and Hakim 2009, 2010, 2012, 2013)



(left) Dynamic tropopause (DT) wind speed (every 15 m s^{-1} starting at 50 m s^{-1} , thick contours) and DT potential temperature (K, thin contours and shading) on 1.5-PVU surface valid at 0000 UTC 1 Dec 1991; **(right)** same as left except DT pressure (hPa, thin contours and shading).

Adapted from Fig. 11 in Pyle et al. (2004).

Motivation

- TPVs may interact with and strengthen jet streams, and act as precursors to the development of intense Arctic cyclones (e.g., Tao et al. 2017)
- Arctic cyclones may be associated with strong surface winds and poleward advection of warm, moist air, contributing to reductions in Arctic sea-ice extent (e.g., Zhang et al. 2013)
- Heavy precipitation, strong surface winds, and large waves accompanying Arctic cyclones may pose hazards to ships navigating through open passageways in the Arctic Ocean

The Great Arctic Cyclone of August 2012 (AC12)

- AC12 formed over Siberia on 2 August 2012 and tracked northeastward into the Arctic, reaching a minimum central sea level pressure (SLP) of 962.3 hPa at 1000 UTC 6 August in the ERA5
- Strong surface winds and waves associated with AC12 helped break up thin sea ice (e.g., Parkinson and Comiso 2013)
- Strong surface winds and waves associated with AC12 also contributed to increased upward ocean heat transport and bottom melting of ice, with sea-ice volume decreasing twice as fast as normal during AC12 (e.g., Zhang et al. 2013)

The Great Arctic Cyclone of August 2012 (AC12)

- Simmonds and Rudeva (2012), Yamazaki et al. (2015), and Tao et al. (2017) found that a TPV played an important role in the life cycle of AC12

The Great Arctic Cyclone of August 2012 (AC12)

- Yamagami et al. (2018) examined the medium-range forecast skill of AC12 with five operational ensemble prediction systems
- They found that AC12 has relatively low predictability, with accurate forecasts of AC12 only out to 2–3 d lead time prior to peak intensity of AC12
- They also found that a more-accurate prediction of upper-level features, including TPVs, in the vicinity of AC12 results in a more-accurate prediction of AC12

The Great Arctic Cyclone of August 2012 (AC12)

- This presentation examines linkages between TPVs and AC12, and the impact of AC12 on Arctic sea-ice extent

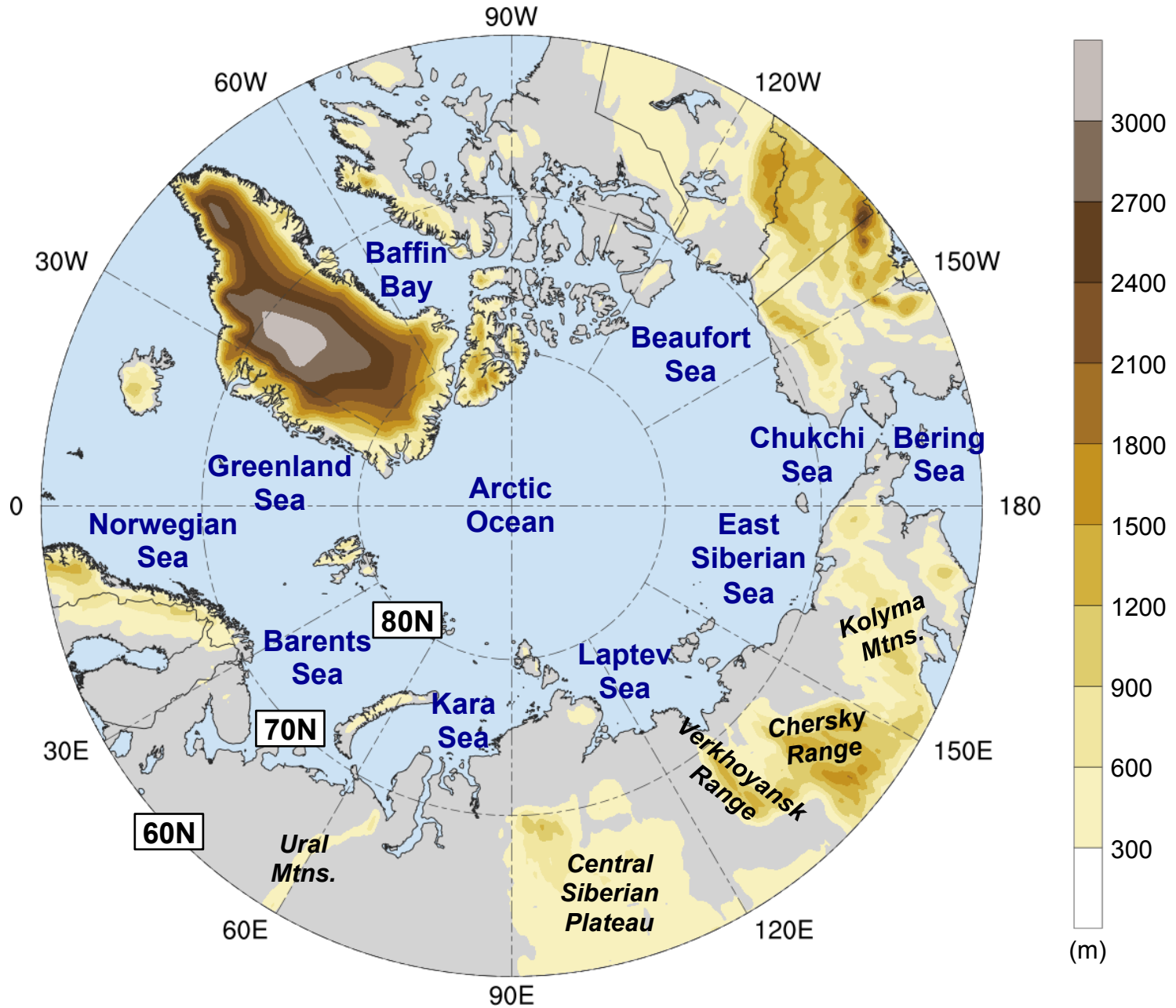
Outline

- Identification and synoptic examination of three TPVs, a predecessor surface cyclone (L1), and AC12
- Impact of AC12 on Arctic sea-ice extent

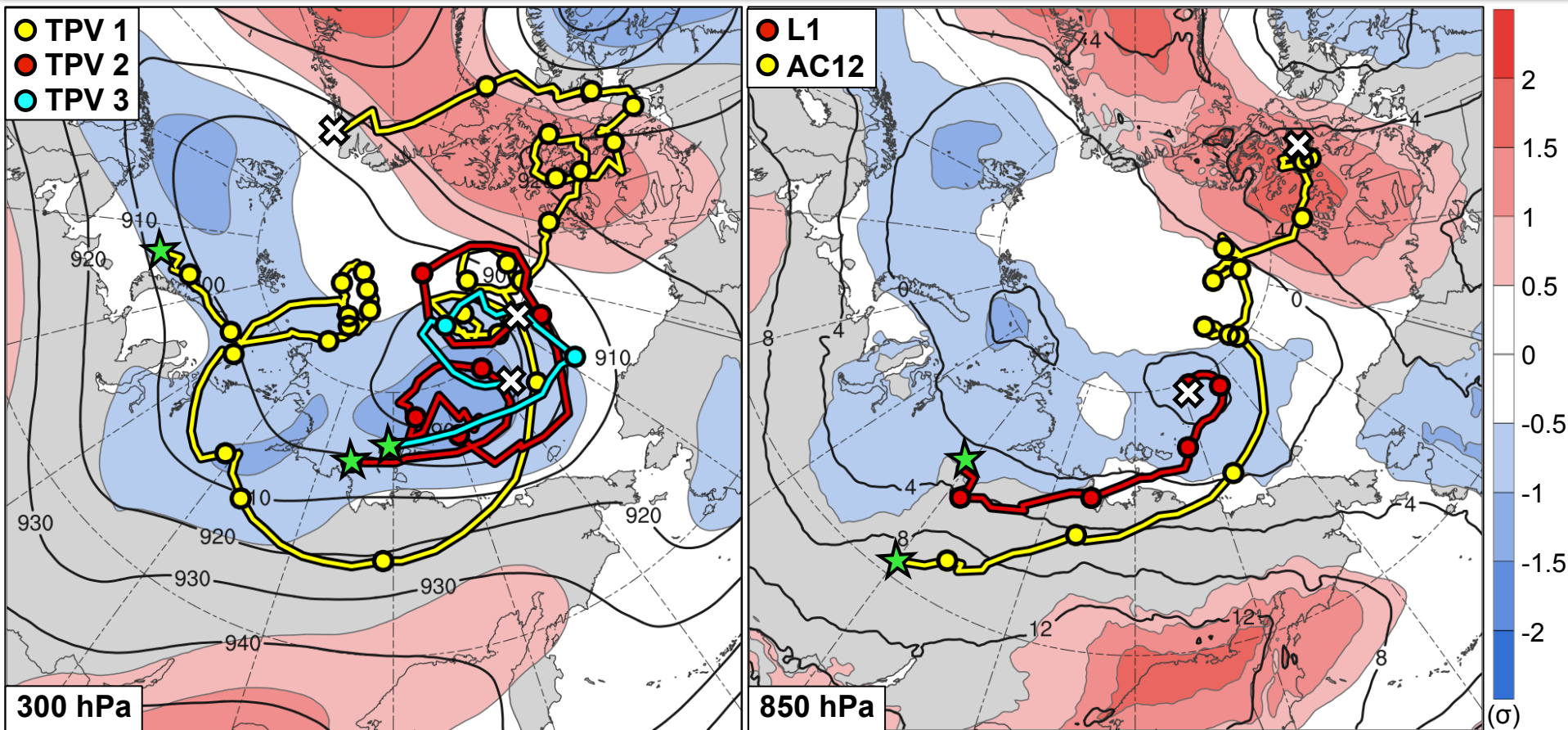
Data and Methods

- Data: ERA5 (Hersbach and Dee 2016) gridded to 0.3° horizontal resolution
- Identified and tracked TPVs of interest for AC12 objectively by utilizing a TPV tracking algorithm (Szapiro and Cavallo 2018)
- Tracked L1 and AC12 manually by following the locations of minimum SLP

Arctic Geography



Track and Intensity



Feature	Genesis	Lysis	Lifetime
TPV 1	23 July	19 Aug	~27 d
TPV 2	3 Aug	9 Aug	~6 d
TPV 3	4 Aug	6 Aug	~3 d
L1	31 July	5 Aug	~5 d
AC12	2 Aug	15 Aug	~13 d

★ Genesis
 ✕ Lysis
 ○ 0000 UTC positions

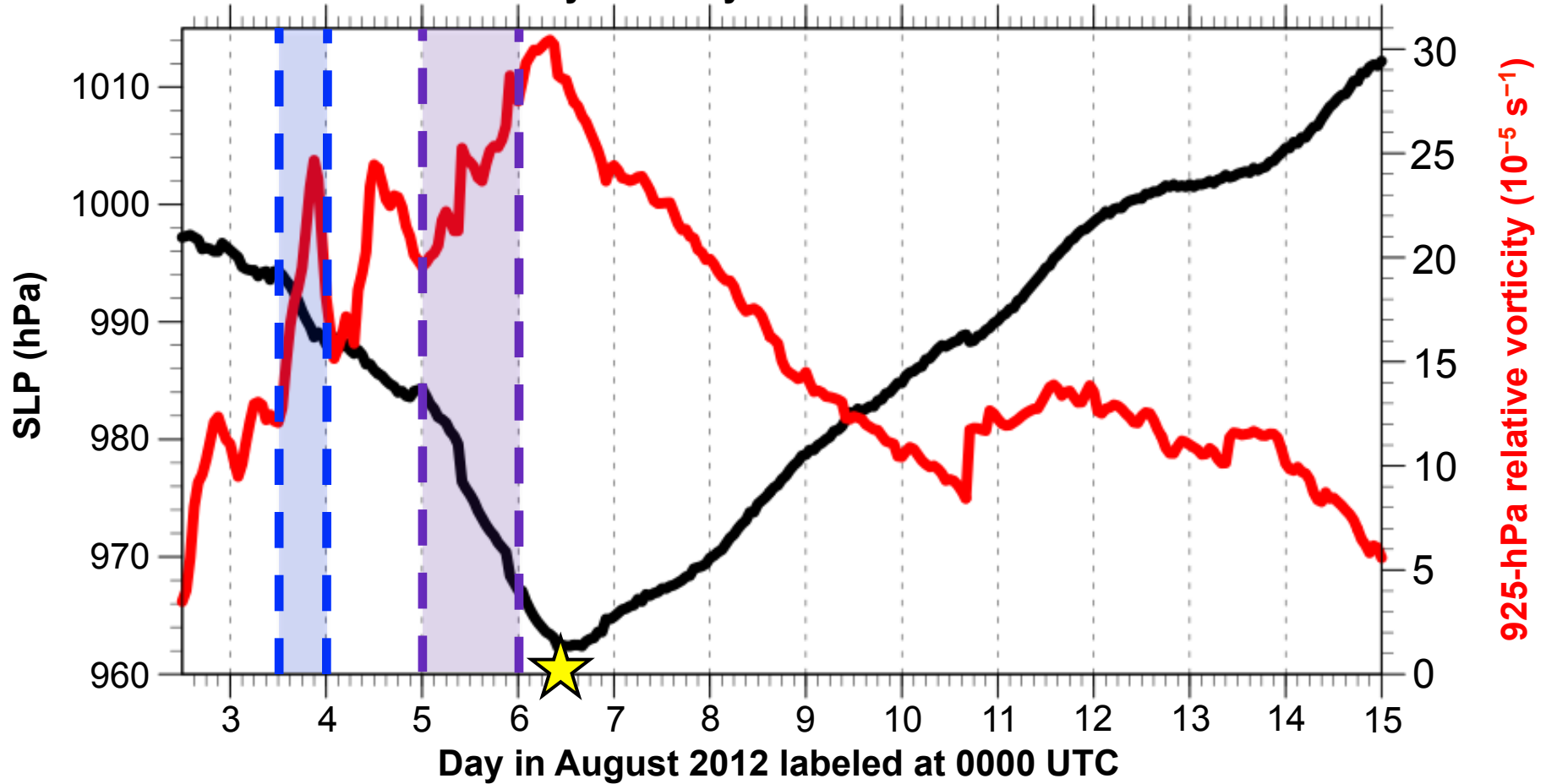
1–7 Aug 2012 time-mean (left) 300-hPa geopotential height (dam, black) and standardized geopotential height anomalies (σ , shaded); (right) 850-hPa temperature ($^{\circ}\text{C}$, black) and standardized temperature anomalies (σ , shaded)

Track and Intensity

- TPV 1 is the longest-lived of the three TPVs and corresponds to the TPV shown in previous studies to play an important role in the evolution of AC12
- TPV 2 and TPV 3 are shorter-lived TPVs and play supporting roles in the evolution of AC12
- L1 is the predecessor cyclone that interacts and merges with AC12
- AC12 is the main cyclone of interest and has a lifetime of ~13 days
- TPV 1 and AC12 track in a region of tropospheric-deep baroclinicity over Siberia

Track and Intensity

Hourly intensity time series of AC12



— Minimum SLP (hPa)

— Maximum 925-hPa relative vorticity (averaged within 100 km of grid point)



Jet coupling phase

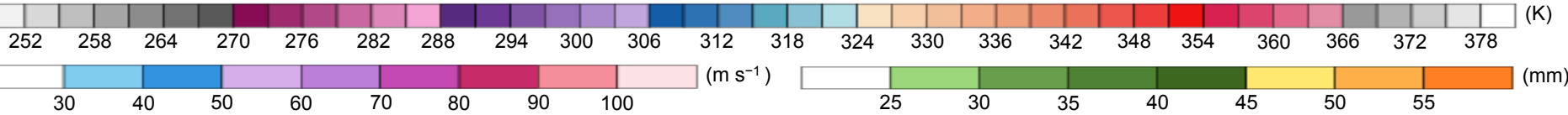
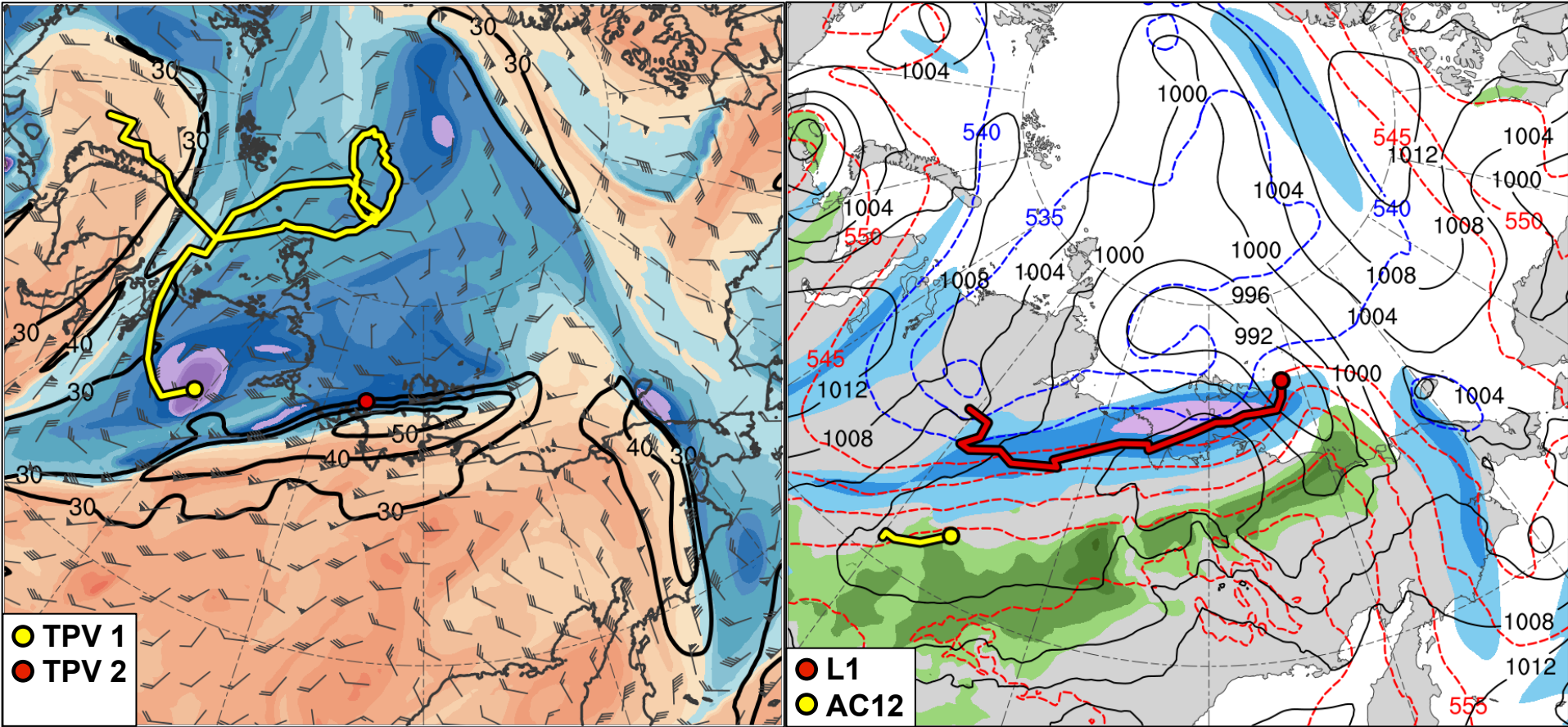
Jet crossing phase



Peak intensity at 1000 UTC 6 Aug 2012 (962.3 hPa)

Synoptic Evolution

0000 UTC 3 Aug 2012

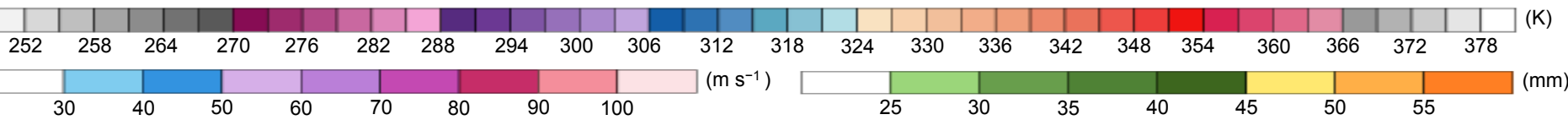
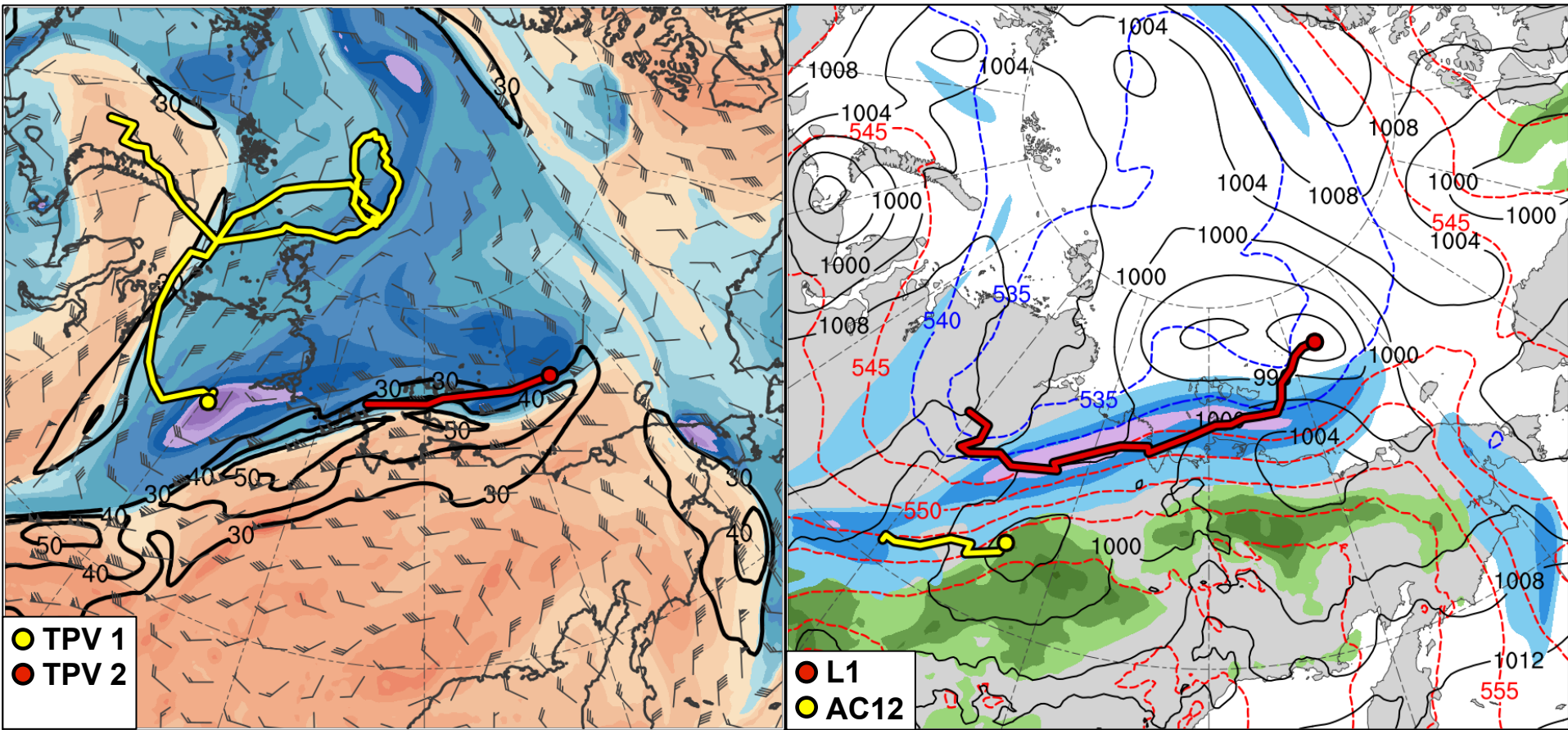


Potential temperature (K, shaded), wind speed (black, every 10 m s⁻¹ starting at 30 m s⁻¹), and wind (m s⁻¹, flags and barbs) on 2-PVU surface

300-hPa wind speed (m s⁻¹, shaded), 1000–500-hPa thickness (dam, blue/red), SLP (hPa, black), and PW (mm, shaded)

Synoptic Evolution

1200 UTC 3 Aug 2012

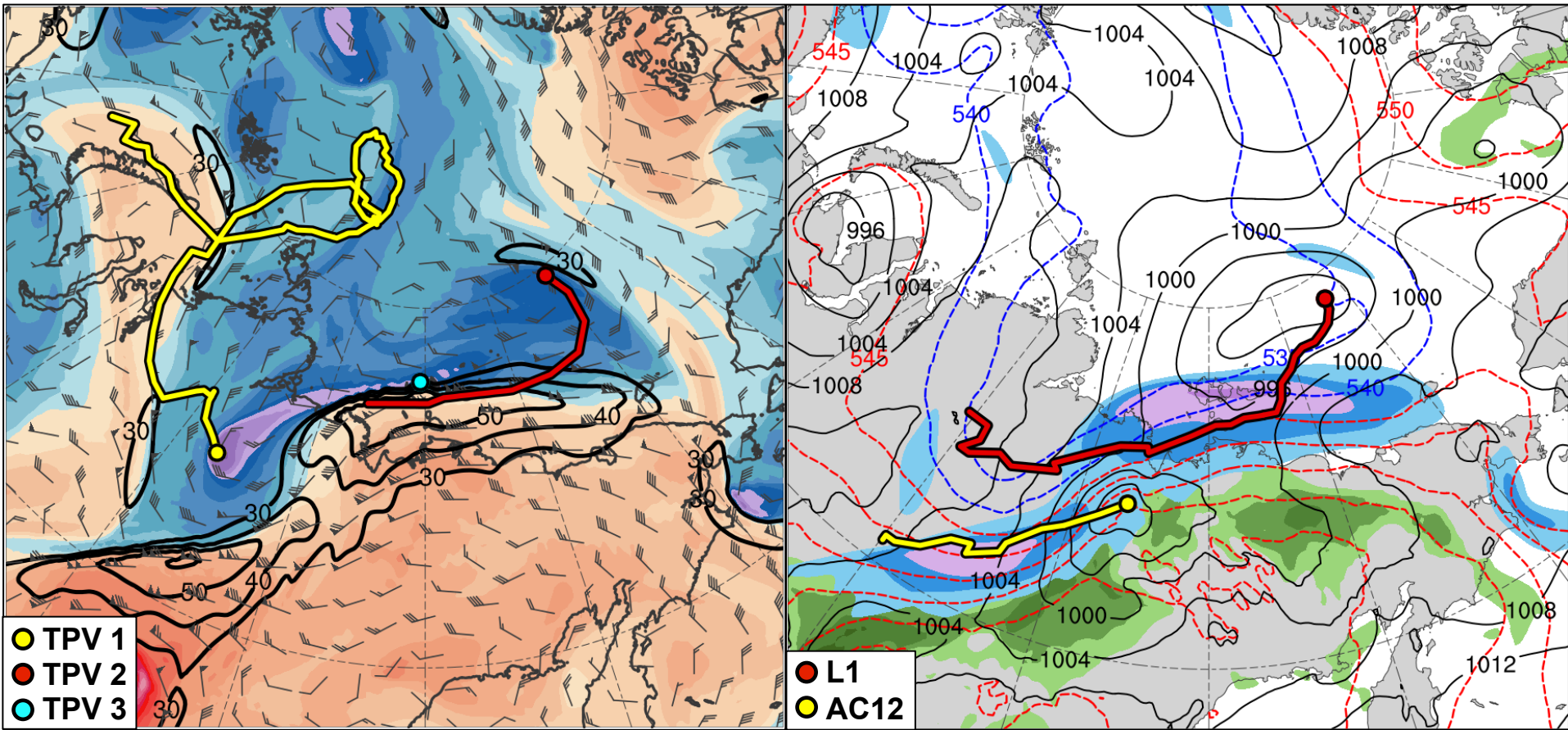


Potential temperature (K, shaded), wind speed (black, every 10 m s⁻¹ starting at 30 m s⁻¹), and wind (m s⁻¹, flags and barbs) on 2-PVU surface

300-hPa wind speed (m s⁻¹, shaded), 1000–500-hPa thickness (dam, blue/red), SLP (hPa, black), and PW (mm, shaded)

Synoptic Evolution

0000 UTC 4 Aug 2012

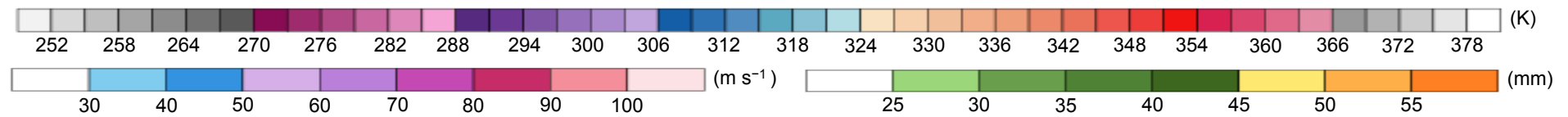
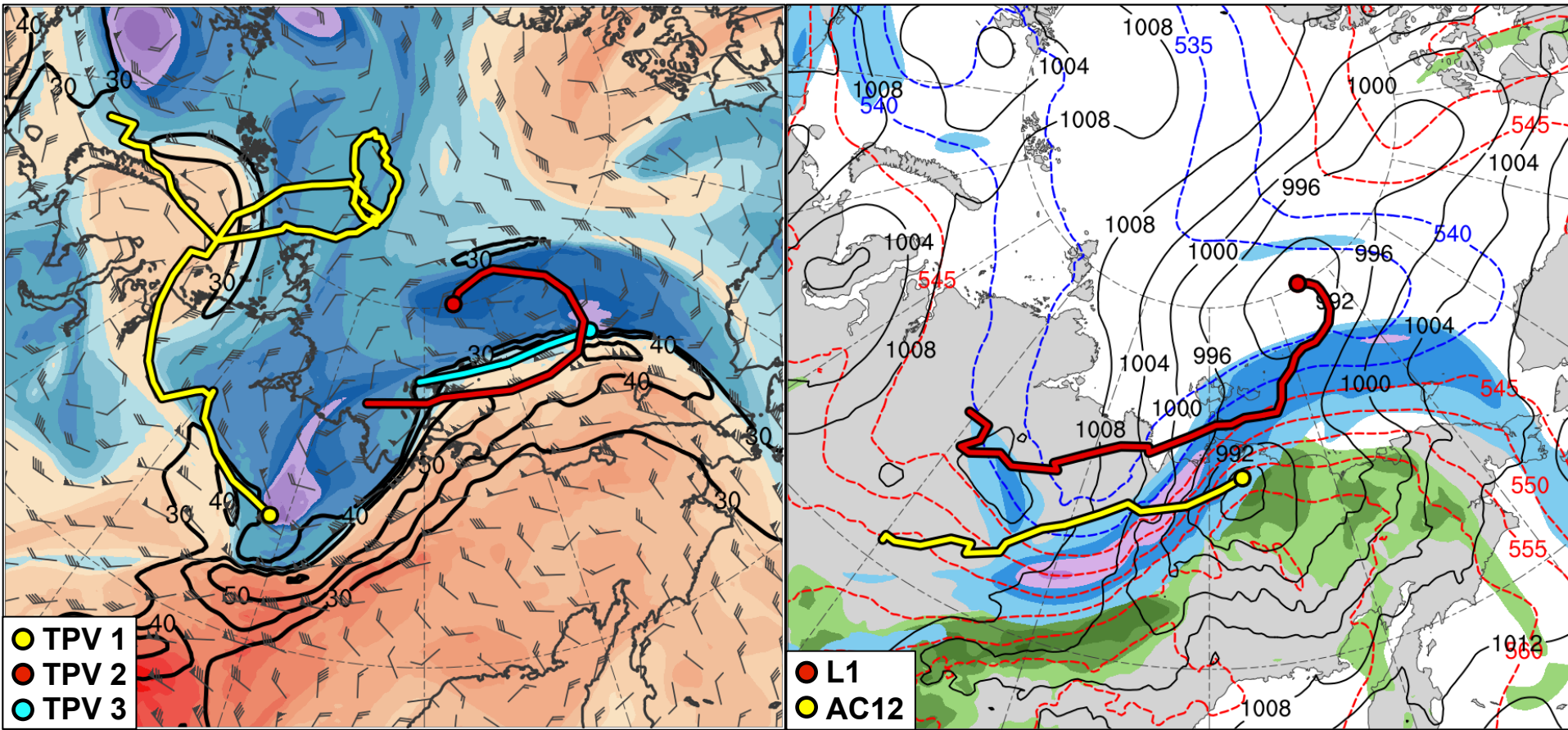


Potential temperature (K, shaded), wind speed (black, every 10 m s⁻¹ starting at 30 m s⁻¹), and wind (m s⁻¹, flags and barbs) on 2-PVU surface

300-hPa wind speed (m s⁻¹, shaded), 1000-500-hPa thickness (dam, blue/red), SLP (hPa, black), and PW (mm, shaded)

Synoptic Evolution

1200 UTC 4 Aug 2012

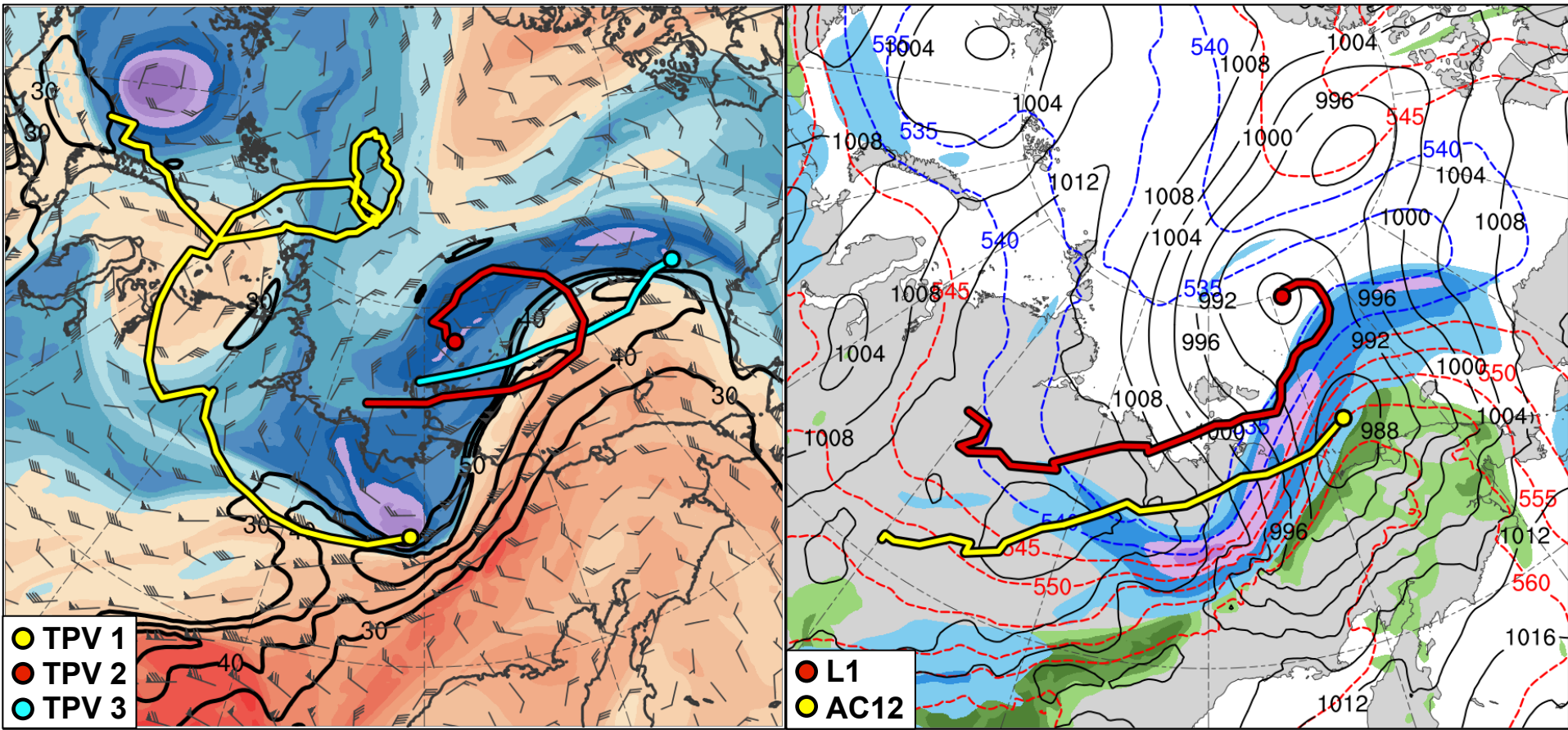


Potential temperature (K, shaded), wind speed (black, every 10 m s⁻¹ starting at 30 m s⁻¹), and wind (m s⁻¹, flags and barbs) on 2-PVU surface

300-hPa wind speed (m s⁻¹, shaded), 1000–500-hPa thickness (dam, blue/red), SLP (hPa, black), and PW (mm, shaded)

Synoptic Evolution

0000 UTC 5 Aug 2012

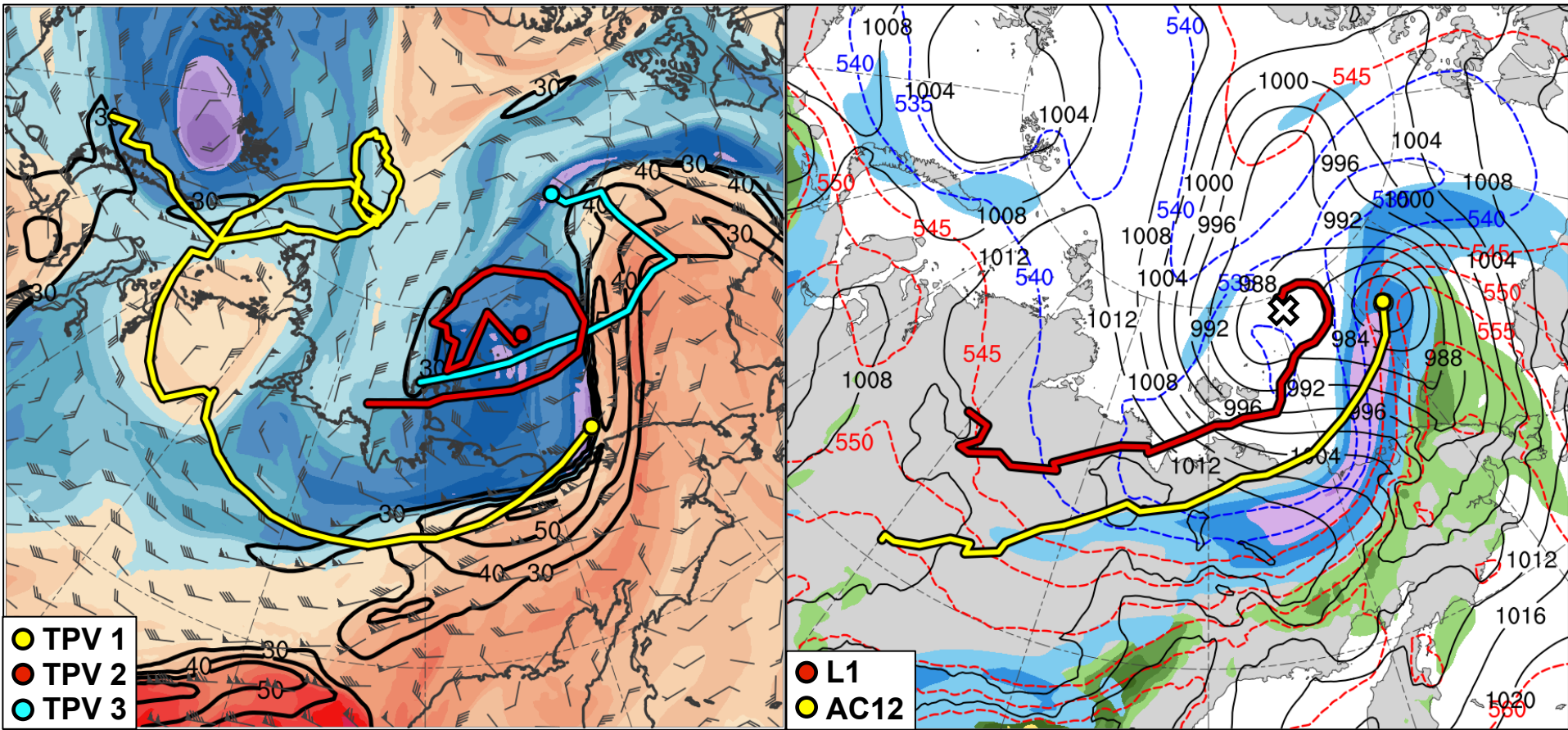


Potential temperature (K, shaded), wind speed (black, every 10 m s⁻¹ starting at 30 m s⁻¹), and wind (m s⁻¹, flags and barbs) on 2-PVU surface

300-hPa wind speed (m s⁻¹, shaded), 1000-500-hPa thickness (dam, blue/red), SLP (hPa, black), and PW (mm, shaded)

Synoptic Evolution

1200 UTC 5 Aug 2012

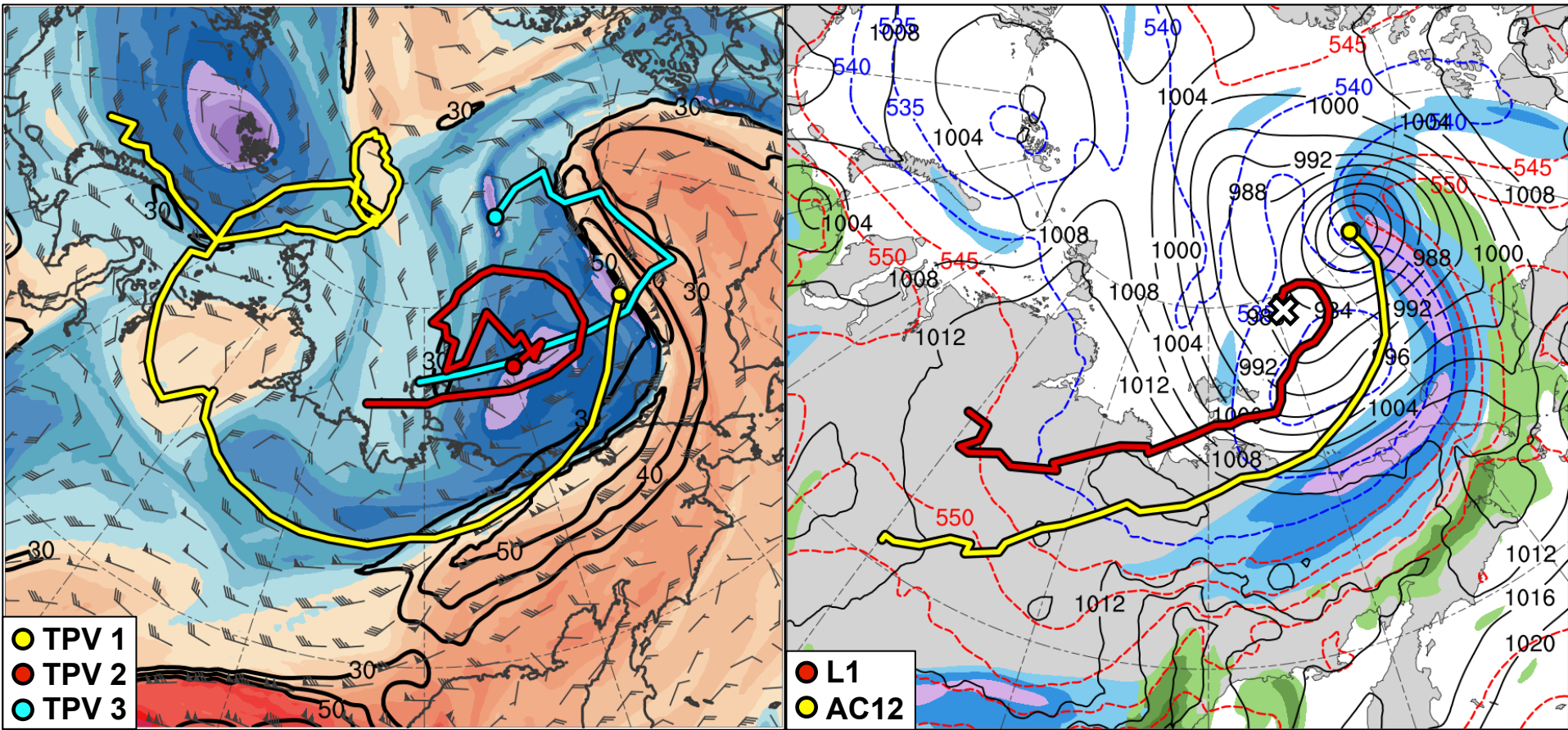


Potential temperature (K, shaded), wind speed (black, every 10 m s⁻¹ starting at 30 m s⁻¹), and wind (m s⁻¹, flags and barbs) on 2-PVU surface

300-hPa wind speed (m s⁻¹, shaded), 1000-500-hPa thickness (dam, blue/red), SLP (hPa, black), and PW (mm, shaded)

Synoptic Evolution

0000 UTC 6 Aug 2012

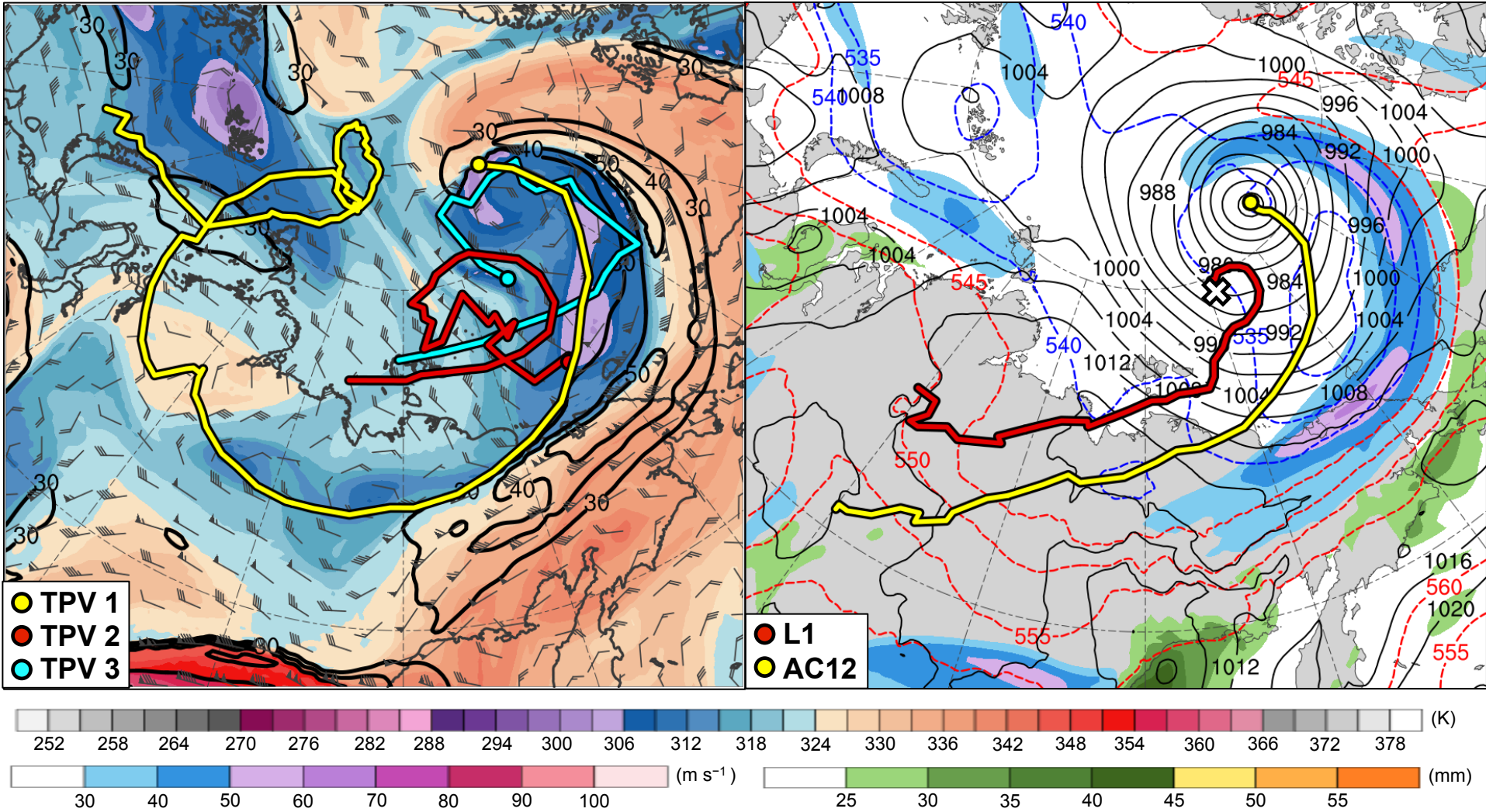


Potential temperature (K, shaded), wind speed (black, every 10 m s⁻¹ starting at 30 m s⁻¹), and wind (m s⁻¹, flags and barbs) on 2-PVU surface

300-hPa wind speed (m s⁻¹, shaded), 1000–500-hPa thickness (dam, blue/red), SLP (hPa, black), and PW (mm, shaded)

Synoptic Evolution

1200 UTC 6 Aug 2012

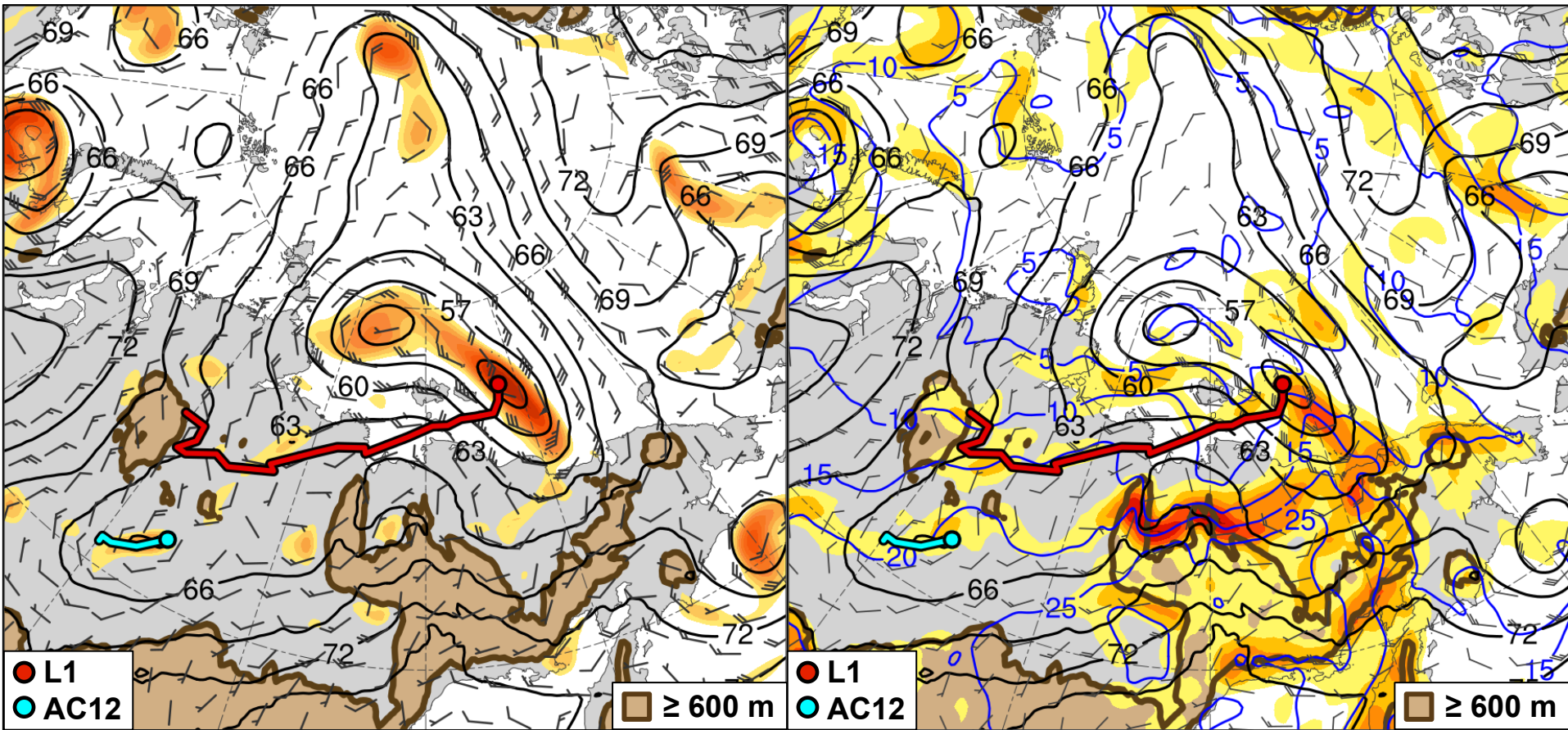


Potential temperature (K, shaded), wind speed (black, every 10 m s⁻¹ starting at 30 m s⁻¹), and wind (m s⁻¹, flags and barbs) on 2-PVU surface

300-hPa wind speed (m s⁻¹, shaded), 1000–500-hPa thickness (dam, blue/red), SLP (hPa, black), and PW (mm, shaded)

Synoptic Evolution

0000 UTC 3 Aug 2012



4 6 8 10 12 14 16 18 20 22 24 26 28

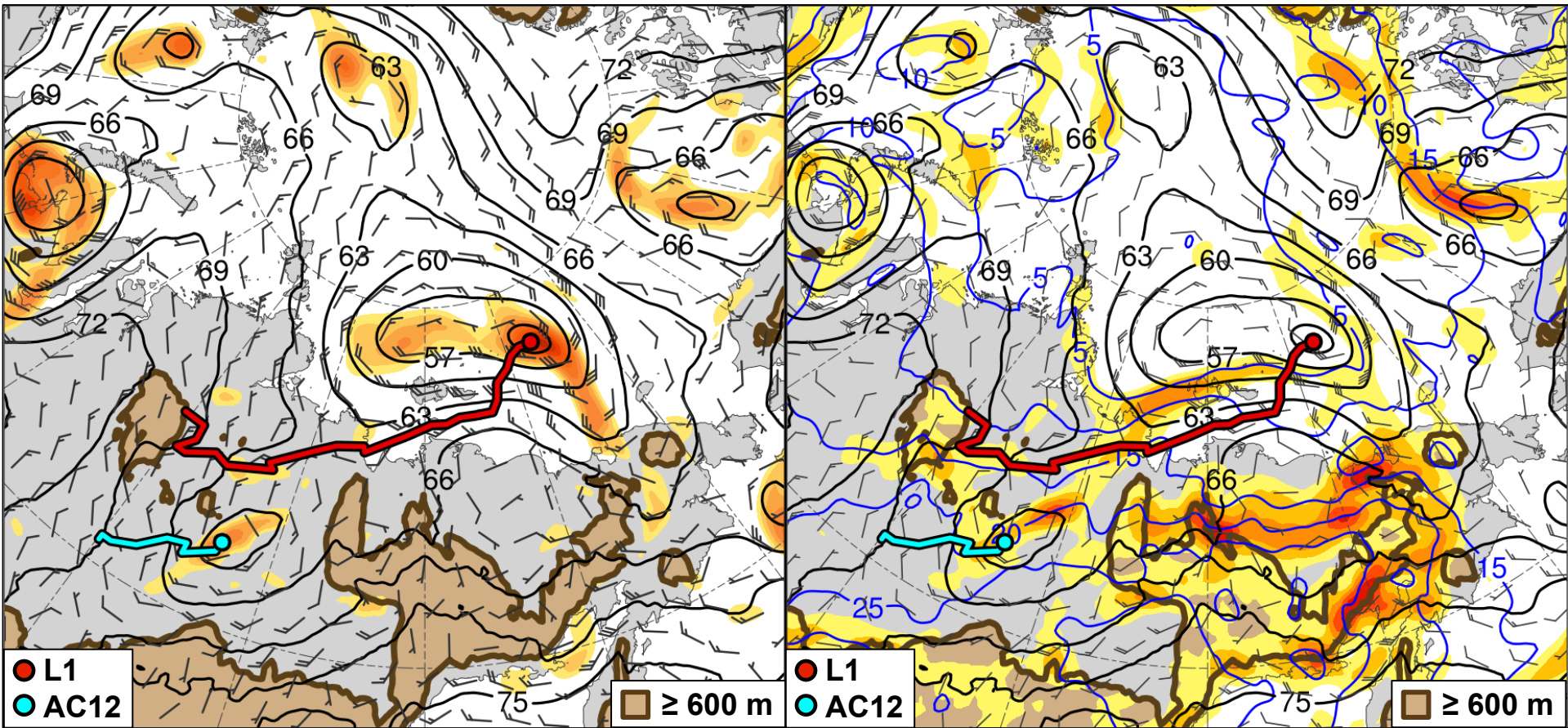
925-hPa area-averaged (100 km) relative vorticity (10^{-5} s^{-1} , shaded), geopotential height (dam, black), and wind (m s^{-1} , flags and barbs)

2 3 4 5 6 7

925-hPa area-averaged (100 km) θ gradient [K (100 km)^{-1} , shaded], θ ($^{\circ}\text{C}$, blue), geopotential height (dam, black), and wind (m s^{-1} , flags and barbs)

Synoptic Evolution

1200 UTC 3 Aug 2012



4 6 8 10 12 14 16 18 20 22 24 26 28

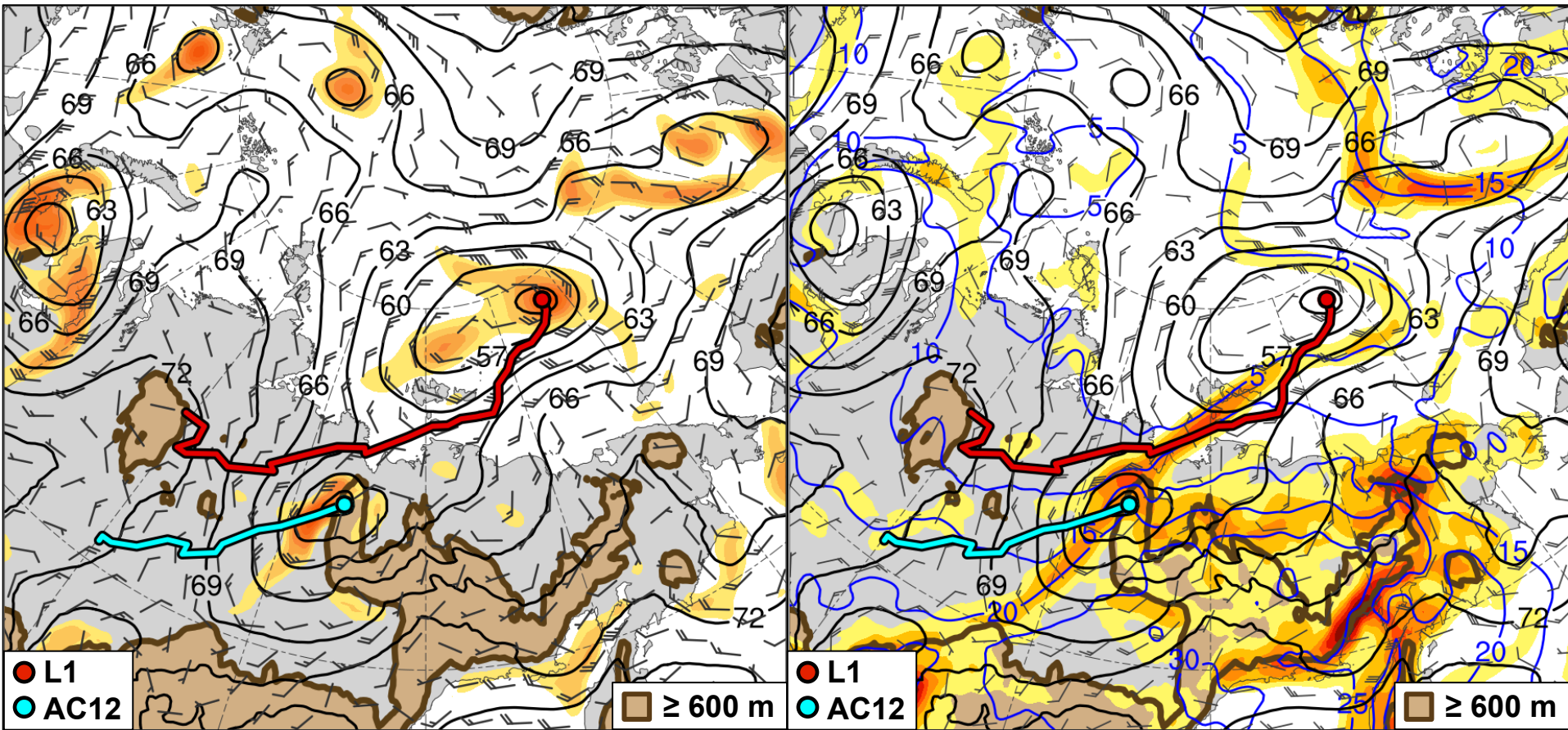
925-hPa area-averaged (100 km) relative vorticity (10^{-5} s^{-1} , shaded), geopotential height (dam, black), and wind (m s^{-1} , flags and barbs)

2 3 4 5 6 7

925-hPa area-averaged (100 km) θ gradient [K (100 km)^{-1} , shaded], θ ($^{\circ}\text{C}$, blue), geopotential height (dam, black), and wind (m s^{-1} , flags and barbs)

Synoptic Evolution

0000 UTC 4 Aug 2012



4 6 8 10 12 14 16 18 20 22 24 26 28

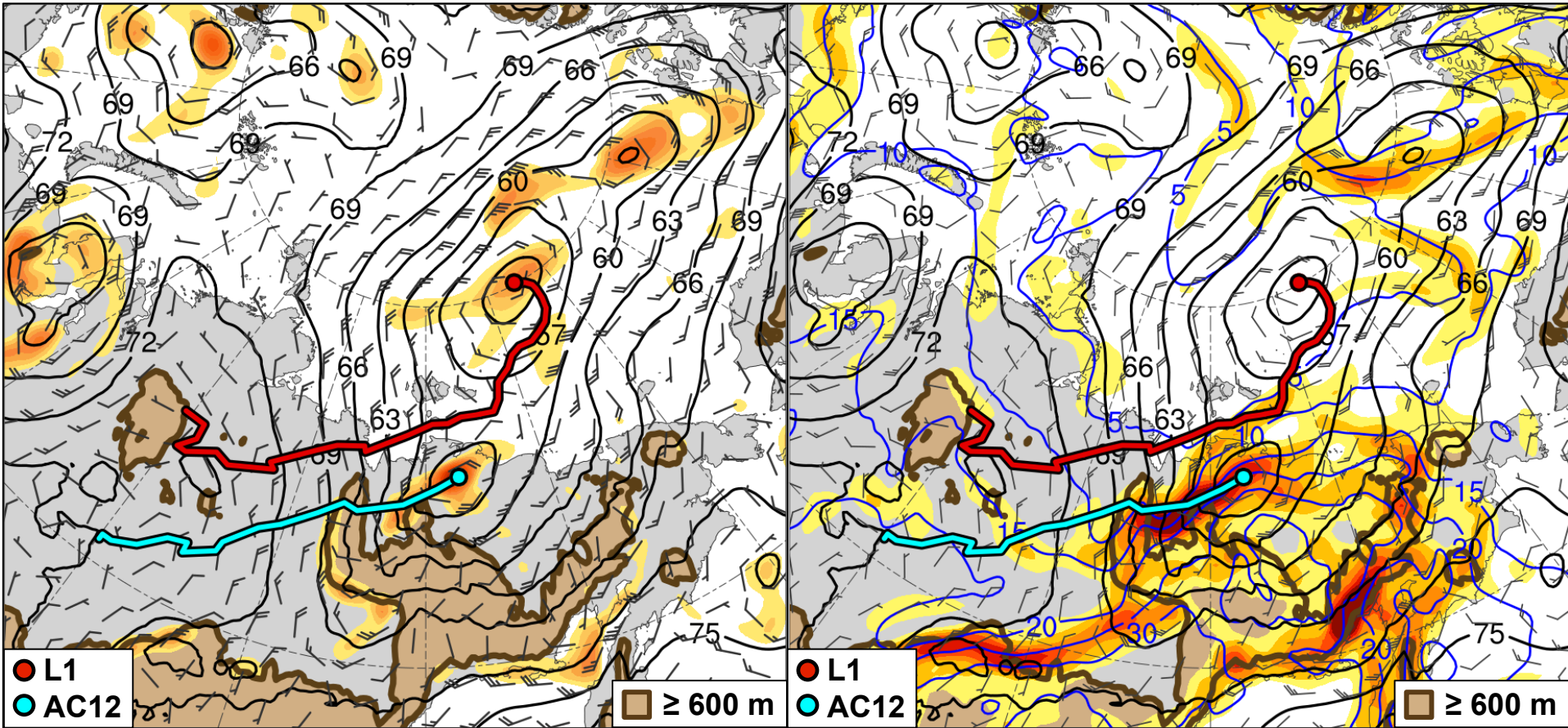
2 3 4 5 6 7

925-hPa area-averaged (100 km) relative vorticity (10^{-5} s^{-1} , shaded), geopotential height (dam, black), and wind (m s^{-1} , flags and barbs)

925-hPa area-averaged (100 km) θ gradient [K (100 km)^{-1} , shaded], θ ($^{\circ}\text{C}$, blue), geopotential height (dam, black), and wind (m s^{-1} , flags and barbs)

Synoptic Evolution

1200 UTC 4 Aug 2012

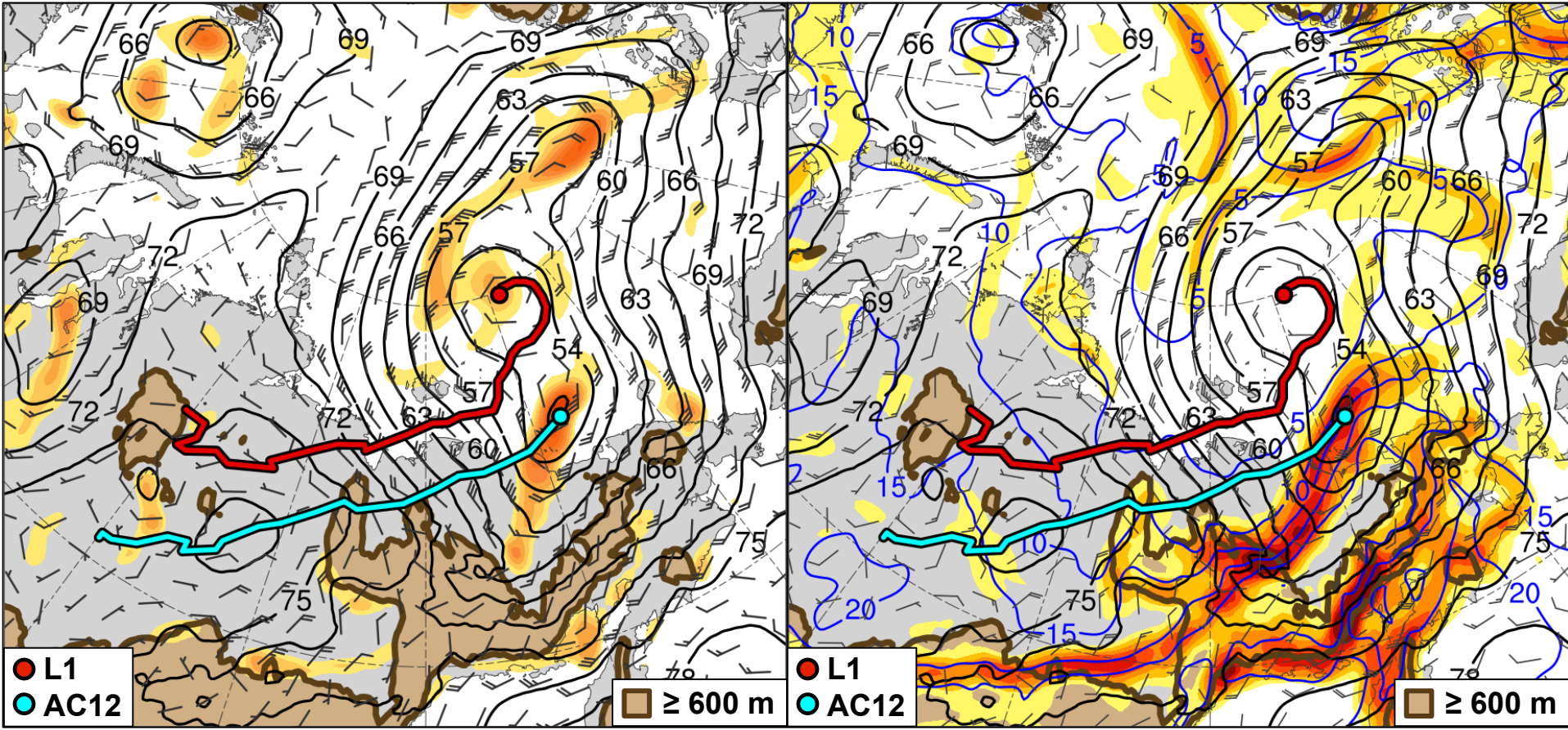


925-hPa area-averaged (100 km) relative vorticity (10^{-5} s^{-1} , shaded), geopotential height (dam, black), and wind (m s^{-1} , flags and barbs)

925-hPa area-averaged (100 km) θ gradient [K (100 km)^{-1} , shaded], θ ($^{\circ}\text{C}$, blue), geopotential height (dam, black), and wind (m s^{-1} , flags and barbs)

Synoptic Evolution

0000 UTC 5 Aug 2012

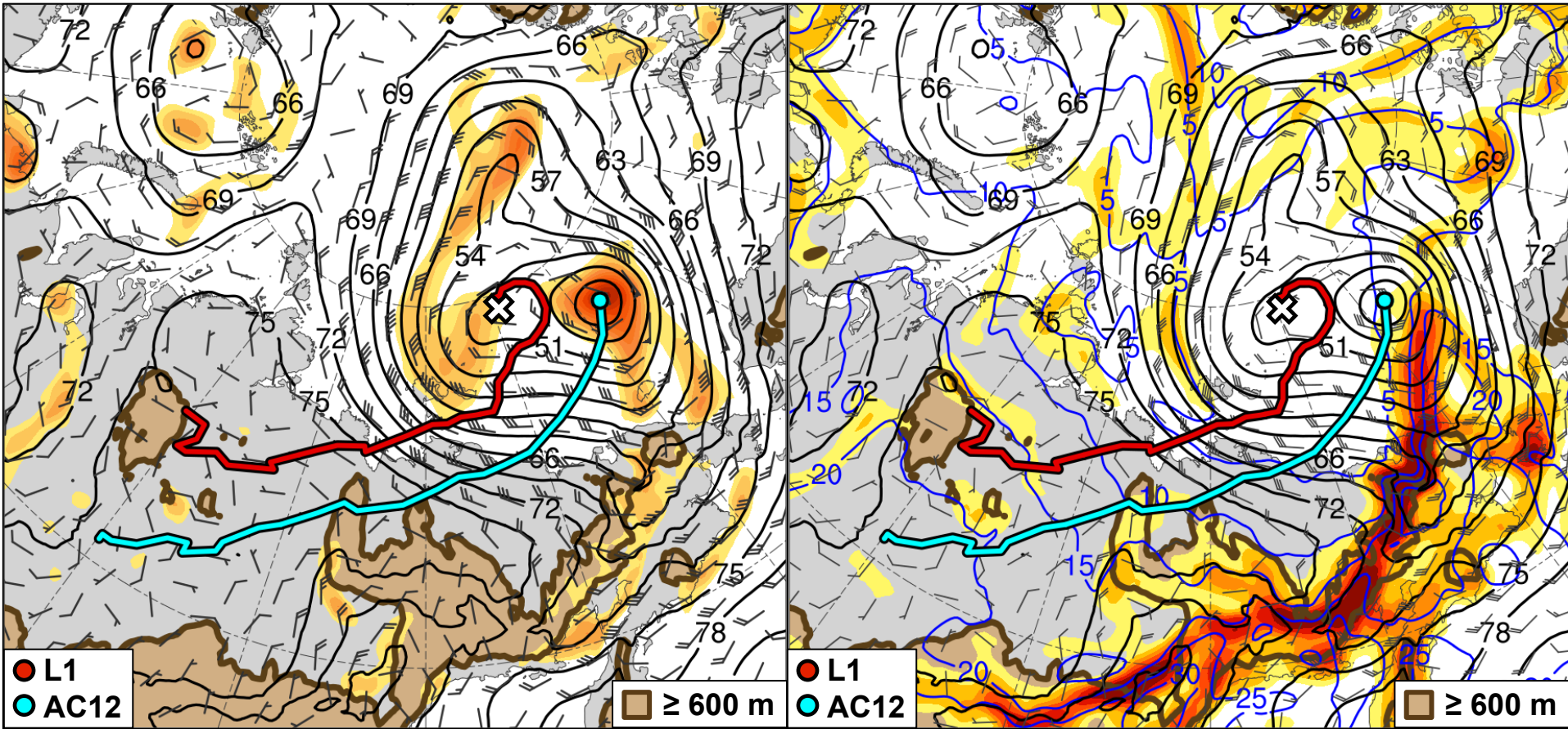


925-hPa area-averaged (100 km) relative vorticity (10^{-5} s^{-1} , shaded), geopotential height (dam, black), and wind (m s^{-1} , flags and barbs)

925-hPa area-averaged (100 km) θ gradient [K (100 km)^{-1} , shaded], θ ($^{\circ}\text{C}$, blue), geopotential height (dam, black), and wind (m s^{-1} , flags and barbs)

Synoptic Evolution

1200 UTC 5 Aug 2012

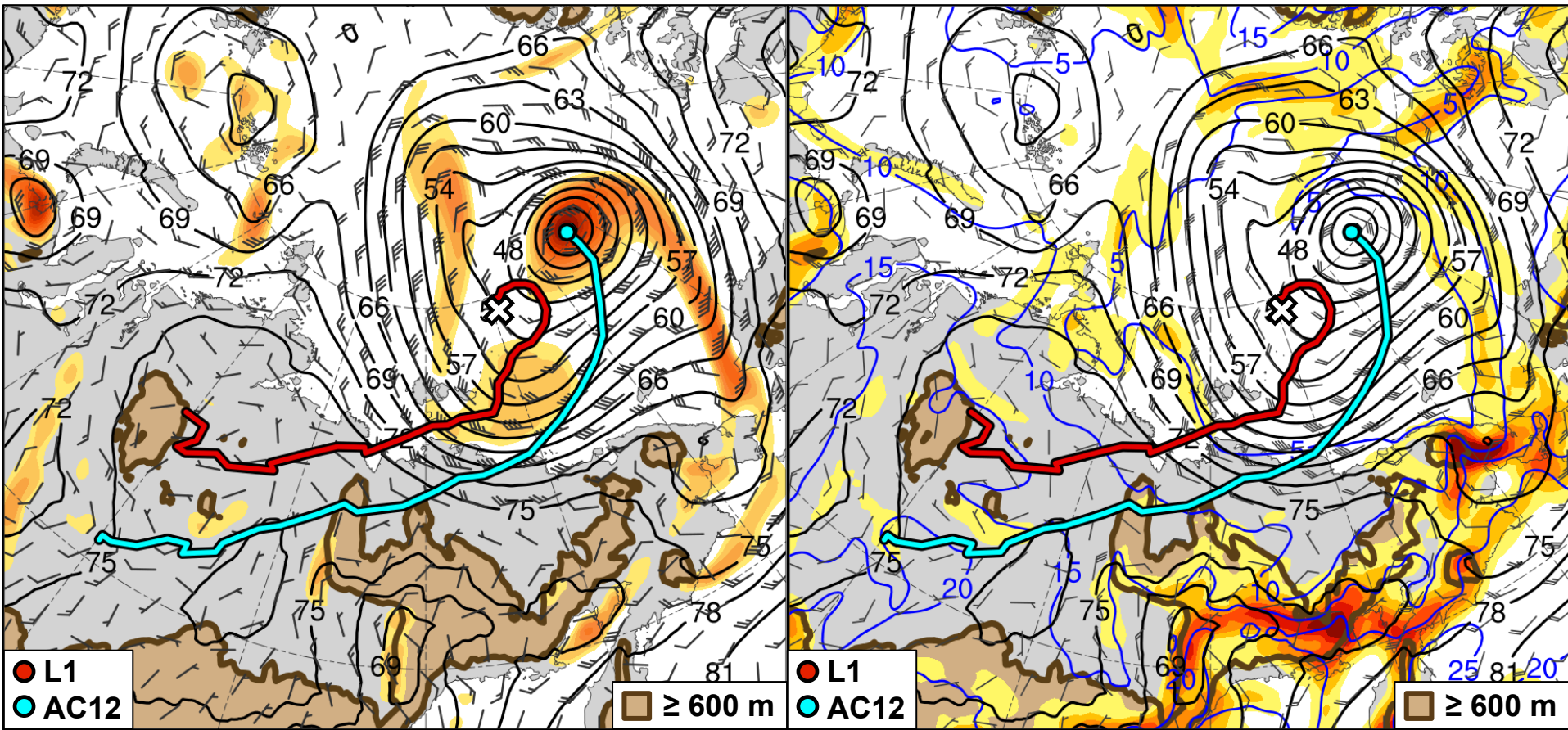


925-hPa area-averaged (100 km) relative vorticity (10^{-5} s^{-1} , shaded), geopotential height (dam, black), and wind (m s^{-1} , flags and barbs)

925-hPa area-averaged (100 km) θ gradient [K (100 km)^{-1} , shaded], θ ($^{\circ}\text{C}$, blue), geopotential height (dam, black), and wind (m s^{-1} , flags and barbs)

Synoptic Evolution

0000 UTC 6 Aug 2012

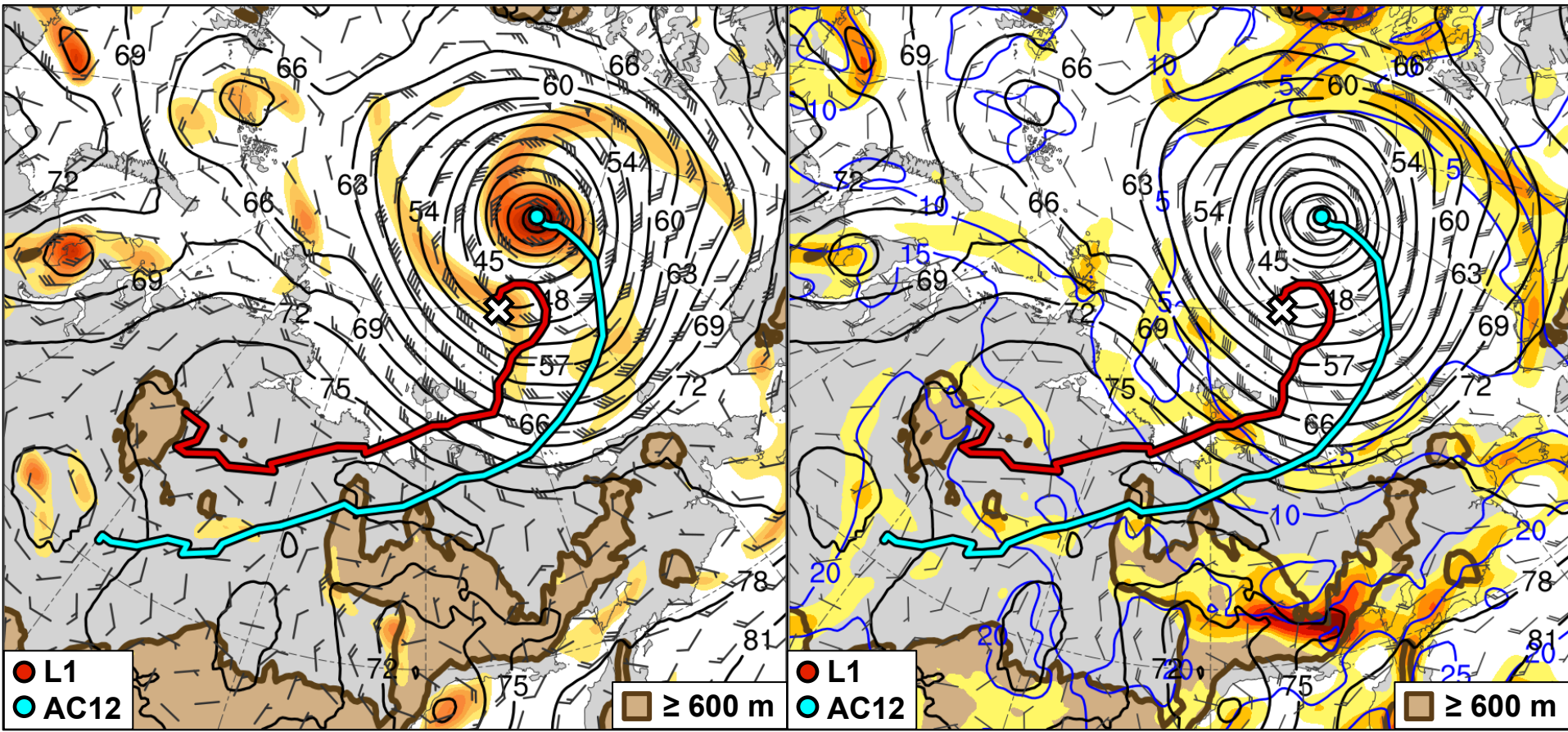


925-hPa area-averaged (100 km) relative vorticity (10^{-5} s^{-1} , shaded), geopotential height (dam, black), and wind (m s^{-1} , flags and barbs)

925-hPa area-averaged (100 km) θ gradient [K (100 km)^{-1} , shaded], θ ($^{\circ}\text{C}$, blue), geopotential height (dam, black), and wind (m s^{-1} , flags and barbs)

Synoptic Evolution

1200 UTC 6 Aug 2012



925-hPa area-averaged (100 km) relative vorticity (10^{-5} s^{-1} , shaded), geopotential height (dam, black), and wind (m s^{-1} , flags and barbs)

925-hPa area-averaged (100 km) θ gradient [K (100 km)^{-1} , shaded], θ ($^{\circ}\text{C}$, blue), geopotential height (dam, black), and wind (m s^{-1} , flags and barbs)

Synoptic Evolution

- TPV 1 approaches and interacts with AC12 in a region of strong baroclinicity, likely supporting the development of AC12 through baroclinic processes
- TPV 2 forms at 0000 UTC 3 Aug east of TPV 1, and TPV 3 forms at 0000 UTC 4 Aug by splitting off from TPV 1
- TPV–jet interactions involving TPV 1, TPV 2, and TPV 3 likely contribute to the formation of a dual-jet configuration and jet coupling over AC12 during 1200 UTC 3 Aug–0000 UTC 4 Aug (jet coupling phase)

Synoptic Evolution

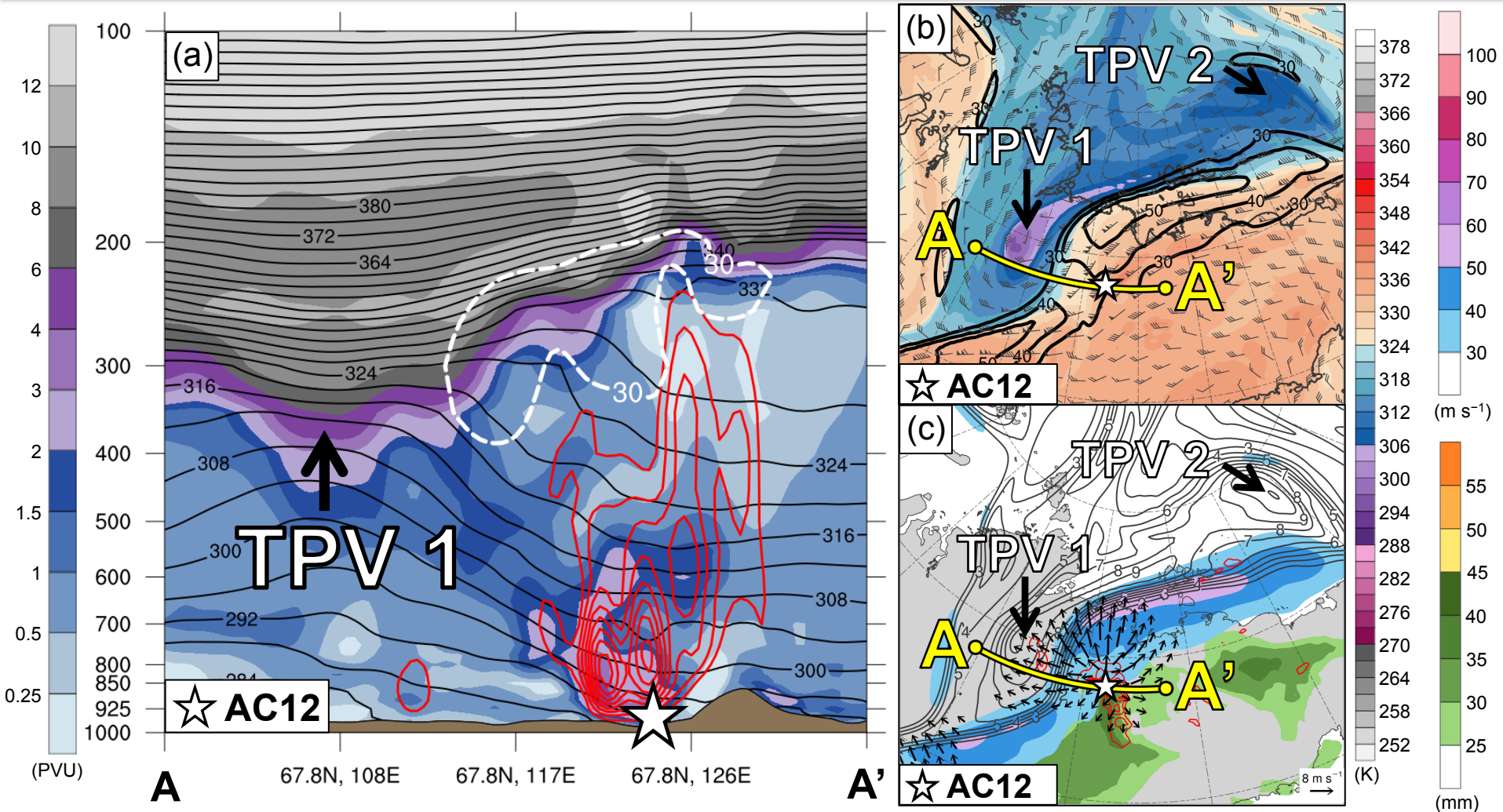
- Upper-level divergence associated with the jet coupling likely supports the intensification of AC12
- The interaction and merger of L1 with AC12 may further support the intensification of AC12
- Cold air advection in the wake of L1 helps maintain the strong baroclinicity in the vicinity of AC12, which also may support the intensification of AC12

Synoptic Evolution

- Most rapid intensification of AC12 occurs during 0000 UTC 5 Aug–0000 UTC 6 Aug, when AC12 crosses from the warm side to the cold side of a strong upper-level jet streak (jet crossing phase)
- AC12 attains peak intensity of 962.3 hPa at 1000 UTC 6 Aug in the ERA5 and becomes vertically aligned with TPV 1 by 1200 UTC 6 Aug
- AC12 and TPV 1 then meander slowly in tandem over the Arctic, while AC12 slowly weakens

Cross Sections: Jet Coupling

2100 UTC 3 Aug 2012



(a) PV (PVU, shaded), θ (K, black), ascent (red, every $5 \times 10^{-3} \text{ hPa s}^{-1}$), and wind speed (white, every 10 m s^{-1} starting at 30 m s^{-1}); (b) DT (2-PVU surface) θ (K, shaded), wind speed (black, every 10 m s^{-1} starting at 30 m s^{-1}), and wind (m s⁻¹, flags and bars); (c) 350–250-hPa PV (PVU, gray) and irrot. wind (m s⁻¹, vectors), 300-hPa wind speed (m s⁻¹, shaded), 800–600-hPa ascent (red, every $5 \times 10^{-3} \text{ hPa s}^{-1}$), and PW (mm, shading)

Cross Sections

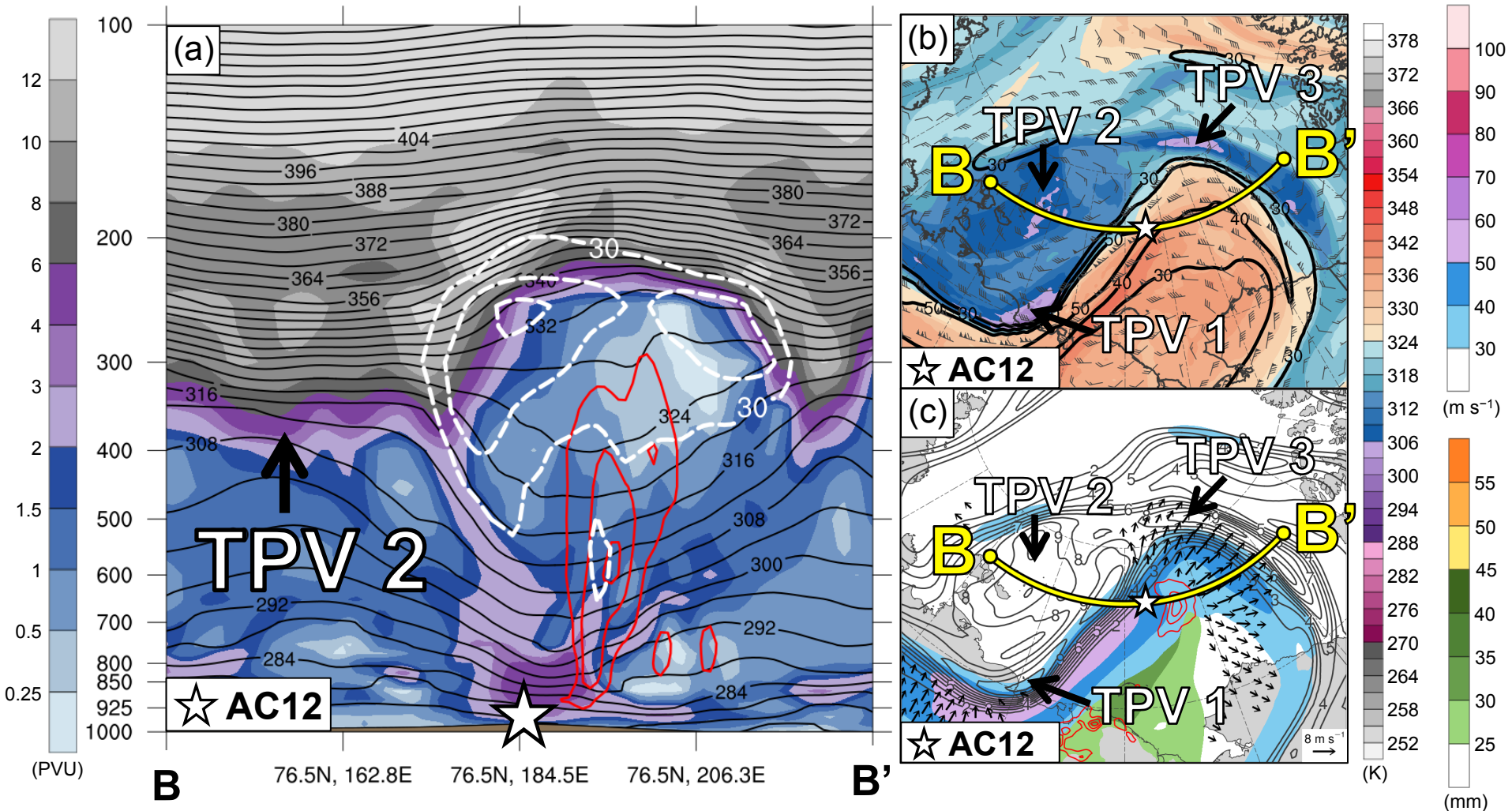
- At 2100 UTC 3 Aug, TPV–jet interactions involving TPV1 and TPV 2 likely contribute to the dual-jet configuration and jet coupling over AC12 (jet coupling phase)
- Jet coupling likely supports relatively strong low-level ascent over AC12
- Latent heating related to the low-level ascent in the presence of warm, moist air likely contributes to the formation of a potential vorticity (PV) tower associated with AC12 and the concomitant intensification of AC12

Cross Sections

- At 2100 UTC 3 Aug, the interaction between TPV 1 and the PV tower also likely supports the intensification of AC12

Cross Sections: Jet Crossing

1200 UTC 5 Aug 2012



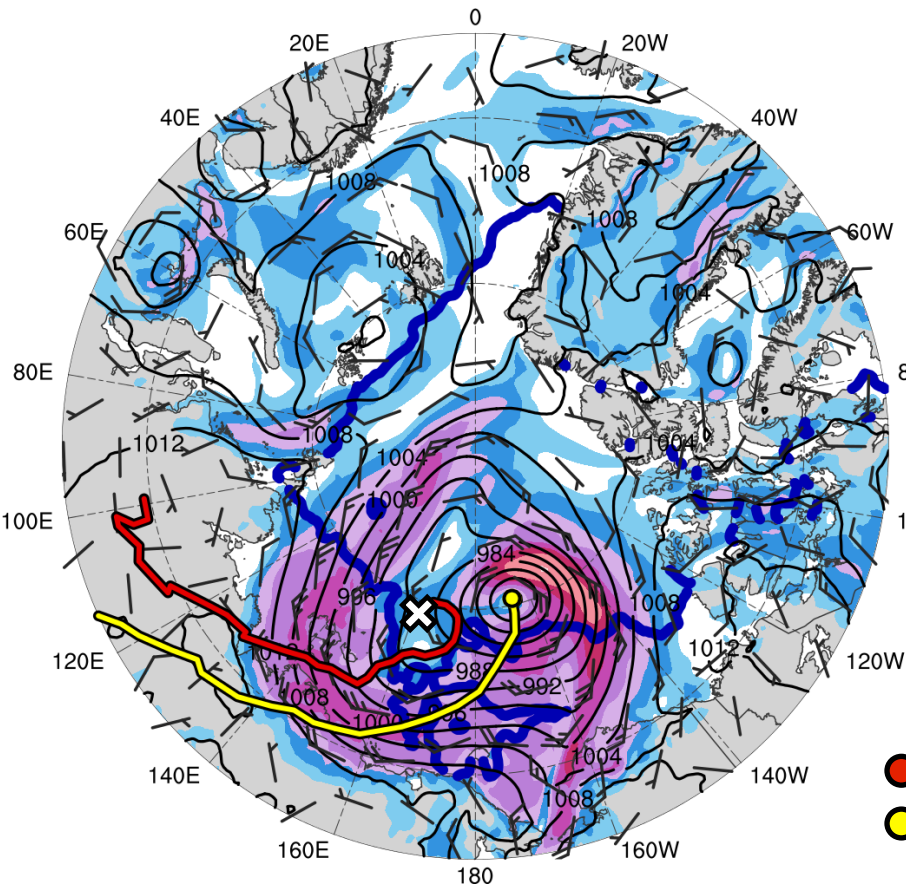
(a) PV (PVU, shaded), θ (K, black), ascent (red, every $5 \times 10^{-3} \text{ hPa s}^{-1}$), and wind speed (white, every 10 m s^{-1} starting at 30 m s^{-1}); (b) DT (2-PVU surface) θ (K, shaded), wind speed (black, every 10 m s^{-1} starting at 30 m s^{-1}), and wind (m s⁻¹, flags and bars); (c) 350–250-hPa PV (PVU, gray) and irrot. wind (m s⁻¹, vectors), 300-hPa wind speed (m s⁻¹, shaded), 800–600-hPa ascent (red, every $5 \times 10^{-3} \text{ hPa s}^{-1}$), and PW (mm, shading)

Cross Sections

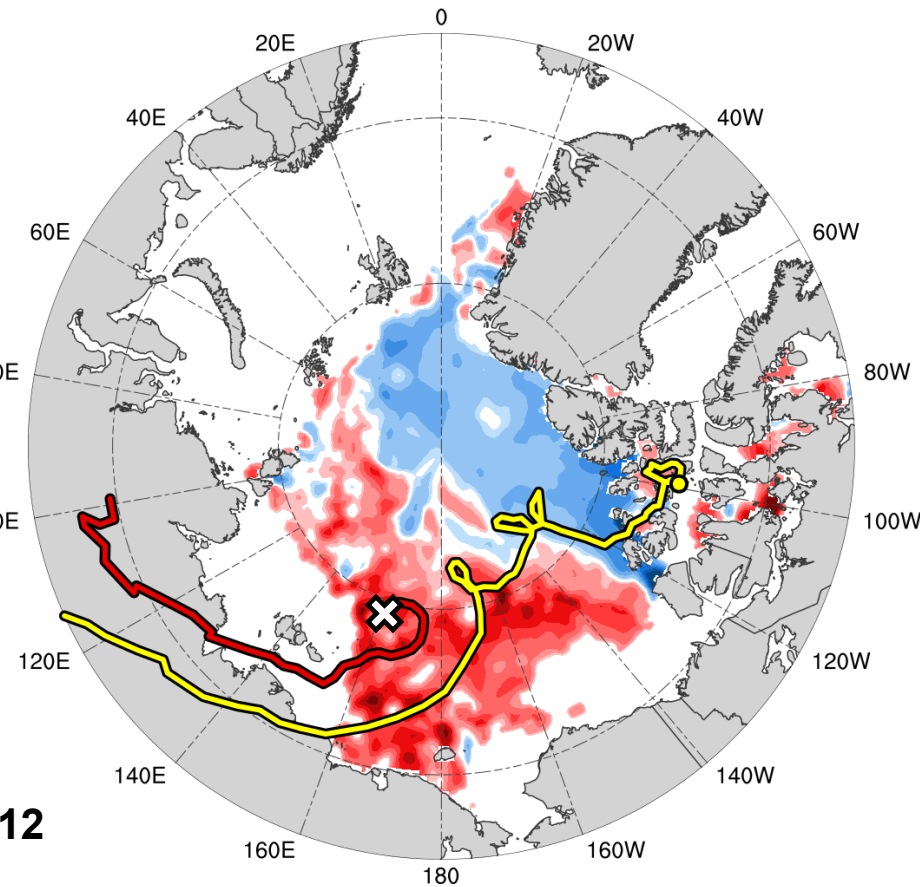
- At 1200 UTC 5 Aug, latent heating likely contributes to the maintenance of the PV tower associated with AC12 and the intensification of AC12 (jet crossing phase)
- The contribution of latent heating at 1200 UTC 5 Aug (jet crossing phase) likely is smaller than at 2100 UTC 3 Aug (jet coupling phase)

Impacts of AC12 on Arctic Sea Ice

0000 UTC 6 Aug 2012



0000 UTC 15 Aug 2012



● L1
● AC12

4 6 8 10 12 14 16 18 (m s⁻¹)

-60 -50 -40 -30 -20 -10 -5 5 10 20 30 40 50 60 (%)

SLP (hPa, black); 10-m wind speed (m s⁻¹, shaded) and wind (m s⁻¹, black barbs), and 20% contour of sea-ice concentration (thick blue)

Change in sea-ice concentration (% , shaded) during 0000 UTC 2–0000 UTC 15 Aug 2012

Impacts of AC12 on Arctic Sea Ice

- AC12 is associated with an expansive field of relatively strong winds
- The relatively strong southerly winds to the east of the center of AC12 are approximately perpendicular to the sea-ice edge, likely helping to move and break up the thin sea ice
- AC12 meanders slowly over the Arctic, leading to a prolonged impact on the sea ice, as illustrated by the relatively large reduction in sea-ice concentration northeast of Siberia

Summary

- TPV 1 approaches and interacts with AC12 in a region of strong baroclinicity, likely supporting the development of AC12 through baroclinic processes
- Cold air advection in the wake of L1 helps maintain the strong baroclinicity in the vicinity of AC12, which also may support the intensification of AC12
- TPV–jet interactions involving TPV 1, TPV 2, and TPV 3 likely contribute to the formation of a dual-jet configuration over AC12 during the jet coupling phase

Summary

- Latent heating related to low-level ascent in the presence of warm, moist air in the region of jet coupling likely contributes to the formation of a PV tower associated with AC12 and the concomitant intensification of AC12
- The interaction between TPV 1 and the PV tower during jet coupling also likely supports the intensification of AC12
- The interaction and merger of L1 with AC12 may further support the intensification of AC12

Summary

- Most rapid intensification of AC12 occurs when AC12 crosses from the warm side to the cold side of a strong upper-level jet streak
- Latent heating likely contributes to the maintenance of the PV tower associated with AC12 and the intensification of AC12 during the jet crossing phase
- Widespread, relatively strong surface winds associated with AC12 contribute to a reduction in Arctic sea-ice extent as AC12 meanders slowly over the Arctic

References

- Cavallo, S. M., and G. J. Hakim, 2009: Potential vorticity diagnosis of a tropopause polar cyclone. *Mon. Wea. Rev.*, **137**, 1358–1371.
- —, and —, 2010: Composite structure of tropopause polar cyclones. *Mon. Wea. Rev.*, **138**, 3840–3857.
- —, and —, 2012: Radiative impact on tropopause polar vortices over the Arctic. *Mon. Wea. Rev.*, **140**, 1683–1702.
- —, and —, 2013: Physical mechanisms of tropopause polar vortex intensity change. *J. Atmos. Sci.*, **70**, 3359–3373.
- Hersbach, H., and D. Dee, 2016: ERA5 reanalysis is in production. *ECMWF Newsletter*, No. 147 ECMWF, Reading, United Kingdom, 7. [Available online at www.ecmwf.int/sites/default/files/elibrary/2016/16299-newsletter-no147-spring-2016.pdf.]
- Parkinson, C. L., and J. C. Comiso, 2013: On the 2012 record low Arctic sea ice cover: Combined impact of preconditioning and an August storm. *Geophys. Res. Lett.*, **40**, 1356–1361.
- Pyle, M. E., D. Keyser, and L. F. Bosart, 2004: A diagnostic study of jet streaks: Kinematic signatures and relationship to coherent tropopause disturbances. *Mon. Wea. Rev.*, **132**, 297–319.
- Simmonds, I., and I. Rudeva, 2012: The Great Arctic Cyclone of August 2012. *Geophys. Res. Lett.*, **39**, L23709.
- Szapiro, N., and S. Cavallo, 2018: TPVTrack v1.0: A watershed segmentation and overlap correspondence method for tracking tropopause polar vortices. *Geosci. Model Dev.*, **11**, 5173–5187.
- Tao, W., J. Zhang, Y. Fu, and X. Zhang, 2017: Driving roles of tropospheric and stratospheric thermal anomalies in intensification and persistence of the Arctic Superstorm in 2012. *Geophys. Res. Lett.*, **44**, 10017–10025.
- Yamagami, A., M. Matsueda, and H. L. Tanaka, 2018: Predictability of the 2012 Great Arctic Cyclone on medium-range timescales. *Polar Science*, **15**, 13–23.
- Yamazaki, A., J. Inoue, K. Dethloff, M. Maturilli, and G. König-Langlo, 2015: Impact of radiosonde observations on forecasting summertime Arctic cyclone formation. *J. Geophys. Res. Atmos.*, **120**, 3249–3273.
- Zhang, J., R. Lindsay, A. Schweiger, and M. Steele, 2013: The impact of an intense summer cyclone on 2012 Arctic sea ice retreat. *Geophys. Res. Lett.*, **40**, 720–726.